On bed porosity of multisized spheroidal particles

Da porosidade de partículas esferoidais polidispersas

DOI:10.34117/bjdv8n2-378

Recebimento dos originais: 07/01/2022
Aceitação para publicação: 18/02/2022

Diogo Rodrigues Prado
Master in Mineral Engineering
Institution: Federal University of Ouro Preto — UFOP
Primetals Technologies
Address: R. Matias Cardoso, 169/sala 601, Santo Agostinho; Belo Horizonte — MG
Brazil; Zip Code 30170-050
E-mail: pradordiogo@gmail.com

José Aurélio Medeiros da Luz
Dr.; School of Mines
Institution: Federal University of Ouro Preto — UFOP
Address: Campus Universitário da UFOP, Bauxita; Ouro Preto — MG; Brazil
Zip Code 35400-000
E-mail: jaurelio@ufop.edu.br

Felipe de Orquiza Milhomem
Mining and environmental engineer (UFPA); Dr.in Mineral Engineering (UFOP)
Institution: Mining Engineering Department — EM
Address: Campus Universitário da UFOP, Bauxita; Ouro Preto — MG, Brazil
Zip Code 35400-000
E-mail: felipe.milhomem6@gmail.com

Marcos Paulo Salomão Paracampos
Mining engineering degree
Institution: Federal University of Ouro Preto — UFOP
Address: R. Sapucaí, 383, Floresta; Belo Horizonte — MG; Brazil
Zip Code 30150-904
E-mail: mpaulo_salomao@hotmail.com

ABSTRACT

In numerous instances of engineering the problem to quantify the porosity of polydisperse systems arises. Despite its great importance, the theoretical predictability of the bed porosity is still problematic. In the field of ceramics, classically, Furnas' studies on porosity are quoted, where he has studied void fraction resulting from blending two distinct particle sizes in various proportions. Less often, ternary diagrams plotting porosity isovalues for spherical particles beds are used to characterize ternary mixtures of distinct monosized particulate systems (usually in ceramics industry). Although similar studies using polydisperse systems have been conducted, a lot of improvement is yet to be achieved. This article falls in this context and aims at contributing to this field of technical and economic impact. Synthetic samples with controlled particle size distribution were used. The resulting porosity of those glass beads random packs

(mimicking several size distributions described by Rosin–Rammler equation) has been experimentally determined under a standardized compaction level. The main result was to obtain an equation for the porosity forecast for bead beds inside spheroidal containers, as a function of the sharpness parameter, n, from Rosin–Rammler distribution. An accurate extrapolation to systems well described by the Whiten sigmoidal distribution was achieved as well. A generalization of the Ergun equation is presented at the end of the article, as an application example.

Keywords: porosity, granular media, rosin–rammler, random packing.

RESUMO

Em numerosas instâncias da engenharia surge o problema de quantificar a porosidade de sistemas polidispersos. Apesar de sua grande importância, a previsibilidade teórica da porosidade do leito ainda é problemática. No âmbito da cerâmica, classicamente, são citados os estudos de Furnas sobre porosidade, em que a porosidade resultante da mistura de dois tamanhos de partículas distintos em várias proporções ficou estabelecida. Menos frequentemente, os diagramas ternários que fornecem isovalores de porosidade para leitos de partículas esféricas são usados para caracterizar misturas ternárias de sistemas particulados monodispersos distintos. Embora estudos semelhantes com sistemas polidispersos venham sendo realizados, aprimoramentos ainda estão por ser obtidos. Este artigo se enquadra nesse contexto e visa a contribuir neste campo de impacto técnico e econômico. Amostras sintéticas com distribuição granulométrica controlada de partículas esferoidais foram empregadas. A porosidade resultante desses empacotamentos aleatórios de esférulas de vidro (varrendo várias distribuições granulométricas descritas pela equação de Rosin–Rammler) foi determinada experimentalmente sob nível de compactação padronizado. O principal resultado foi obter uma equação para a previsão de porosidade para leitos de esferoides em recipientes esferoidais, em função do parâmetro de agudez, n, da distribuição de Rosin–Rammler. Também foi obtida uma extrapolação acurada para sistemas bem descritos pela distribuição sigmoidal de Whiten. Uma generalização da equação de Ergun é preconizada ao final, a título de exemplo de aplicação.

Palavras-chave: porosidade, meio granular, rosin–rammler, empacotamento aleatório.

1 INTRODUCTION

Granular materials are abundant in nature. There are examples of such systems in the beach sand, in the desert dunes and even in the ice grains that make up the Saturn's rings. Granular materials account for about 75 % of all raw materials in stock and are the second most handled material in the industry, with water being the first one. Granular material handling is always present in mining and metallurgical sectors, mainly in the stacking and reclaim of ore storage and homogenization stockpiles, as well as in hauling by conveyor belts.

Processes that use particulate matter are numerous. In this type of system there are always empty spaces between the particles. The ratio between voids volume and the total

volume occupied by the particles is known as volume porosity, or only porosity for brevity. The desired porosity values vary from instance to instance. Hence, while for some processes, a high amount of porosity results in excellent products, for other ones it may mean a product of poor quality.

Among instances where knowing the value of porosity is essential, one can include: study of reservoir rocks, as a key parameter to evaluates the potential of hydrocarbon concentration in sedimentary rocks; agricultural engineering, as silo design and handling operations are concerned; solid-liquid separation, such as filtration and thickening; geophysical prospecting of lithoclastic deposits (whose porosity may be determined from electrical resistivity measurement); handling of bulk materials, drying processes; froth analysis in industrial flotation machines, metallurgical processes such as pelletizing, sintering and coke production (PÖTTKER; APPOLONI, 2000; ZOU; GAN; YU, 2011).

Furnas, one of the pioneers in the study of granular bed packing, has shown that using two different particle sizes to form a particulate bed, porosity varies by changing the fraction of each particle class in the bed. There is a particular proportion of constituents, which results in minimum value for porosity of the blend (FURNAS, 1928).

In line with this achievement, the case of expansive mortar for fracturing and demolition is an eloquent example in which porosity is a key factor in process performance. When filling holes in a rock mass with this type of fresh mortar, the volumetric expansion resulting from the (kinetically controlled) hydration of the alkaline oxides that compose it must be counteracted by the paucity of interstitial voids in order to transmit powerful traction forces towards the rock mass. Therefore, the proportion of interstitial voids in the mortar must be minimized so that traction is maximized, leading to a controlled rupture of the rock mass, according to the drillhole alignment, as stated by Montenegro-Balarezzo *et al* (MONTENEGRO-BALAREZO; LUZ; PEREIRA, 2003).

In turn, Anderegg assessed the porosity of a particulate system using mortar (mixture of sand, cement, crushed stone, and water), in which the porosity is a decisive factor for the properties of the material because this property impacts both the mortar workability, and in its subsequent mechanical strength (ANDEREGG, 1931).

Although the porosity concept is useful in various fields (thus becoming very important its determination), measuring this parameter is sometimes quite tricky and sometimes contaminated by uncertainties.

A case in which the determination of the porosity is of great importance and also quite complicated is the online determination of porosity of filter cakes (DAS; RAMARAO, 2002). The use of optical or electron microscope to measure this property in the bed under study will usually cause displacement of particles within the bed, which, most likely, will change the value of porosity. An alternative is to embed the material with resin, taking due care to ensure that all spaces are filled and also ensuring any movement of the fluid does not cause the particles to move in the bed Schmidt and Loffler (SCHMIDT; LÖFFLER, 1990),

With regard to idealized monodisperse systems, Scott (1960), using spheres in determining the value of porosity, reached the value of 0.41 for loose packing and 0.37 for the porosity of densified or compacted packing. Spheres of the same size were used in his study. The difference in values is due to the fact that he used vibration for compaction in the second case. Vibration has promoted a better accommodation of particles in order to lower the centroid of that system, resulting in lower values of porosity.

Examples of the importance of porosity can also be attributed to fluid flow inside particle beds (compacted or loose) in 2D or 3D systems. Silva, Geyer and Pantoja (2020) said that porosity is related to performance and durability of the buildings. Dornelas *et al.* (2021) pointed out that in the case of petroleum sector, the permeability of the porous media is an important parameter to be taken into account in the process, and the barium sulfate ($BaSO_4$) precipitation reaction can lead to an increase in pressure in the porous medium. MacDonald *et al* (1979) reviewed the Ergun equation, which is widespread for flow analysis in particulate beds, and empirically investigated the dependence of the equation with porosity, concluding that using $\varepsilon^{3.6}$ instead of ε^3 in the Ergun equation (ε is porosity) results in better data adherence. Das, Deen and Kuipers (2017) performed numerical simulation of heat transfer from a cylindrical reactor filled with spherical particles, and found a relationship between porosity and column diameter/particle diameter ratio. Mueller (2012) , in turn, determined the radial porosity in bed of spheres, according to him, being useful in the representation of transport in beds according to their radial position. In summary, the use of computer simulation to analyze packing problems in granular beds has grown in recent years (CAMPELLO; CASSARES, 2016; POZZOBON; COLIN; PERRÉ, 2018; PRIOR; ALMEIDA; LOUREIRO, 2013; RODRÍGUEZ; ALLIBERT; CHAIX, 1986).

Wang and colleagues (2016), on the other hand, simulated a 2D CFD model of Montan wax extraction, comparing it with a 3D packing model. The authors determined the relationship between global porosity and particle size distribution. This is because, to perform the simulation, they needed to predict the global porosity (across the bed of particles), doing so based on the Trask sorting coefficient (TRASK; HAMMAR; WU, 1932), which is given by the following relationship (Equation 1):

$$T_o = \sqrt{\frac{first\ quartile\ diameter}{third\ quartile\ diameter}} = \sqrt{\frac{x_{25}}{x_{75}}} \quad (1)$$

Where: x_{25} and x_{75} are the particle sizes where 25 % and 75 % of the particle mass respectively are found. Thus, based on the size distribution, according Wang and coworkers (2016), porosity can be given by Equation 2:

$$\varepsilon = 0.7895 - 0.2786 \times T_o \quad (2)$$

Lanfrey, Kuzeljevic and Dudukovic (2010) found a model to describe the tortuosity of compacted particle beds, based on the sphericity of the particles and on a packing factor given as a function of the porosity. According to them, the model found has good correlation with porosities ranging from 0.36 to 0.45.

Dias *et al.* (2006) also studied the tortuosity of particle beds, finding, in turn, the tortuosity both as a function of porosity and of a specific parameter dependent on the bed permeability, showing the interdependence of the various parameters of granular material. In turn, Mota, Teixeira and Yelshin (1999) have proposed the existence of macro and microtortuosity in a bidispersed bed, with each subparameter corresponding to a monodispersed bed. Frery and coworkers, basing on the size distribution and soil porosity, have proposed an algorithm that makes it possible to simulate several system conditions (FRERY *et al.*, 2012). In turn, Burtseva and coworkers (2015) presented an interesting review on the main polydisperse spheres packing models.

In addition to the relationship between porosity and particle packing, many studies have analyzed the transport of heat and mass in particulate beds. Médici and Allen (2016) performed the comparison between experiments and simulation of percolation in porous beds, reaching good correlations. Although the connections among the pores have been

considered as cylindrical ones, they have claimed the technique used can be extended for other types of pore network simulation. Augier, Idoux and Delenne (2010) have carried out CFD simulation of percolation in a well-compacted spherical bed (porosity of 33 %). According to them, the use of CFD was interesting for the study of the transport of heat and mass in a particulate bed, being possible to analyze even the wall effect.

Another problem is the conversion from area to volume which may introduce errors in the analysis. This occurs commonly in determination of porosity by image analysis, since it actually measures the apparent voids ratio in a given section of the particulate bed.

Interesting example of this aspect can be illustrated by the following figure (Figure 1). *IrfanView*, a freeware computational package designed for image editing, was employed to perform an image analysis, alternatively. Using its histogram toolbox to assesses the numeric values of the pixels it was possible to measure the superficial porosity of images in black (value 000) and white (value 255).

Figure 1 — Image histogram for a porous system simulated by Monte Carlo method. The void fraction, showed in black will be: (100 – 63.4) % = 36.6 %.

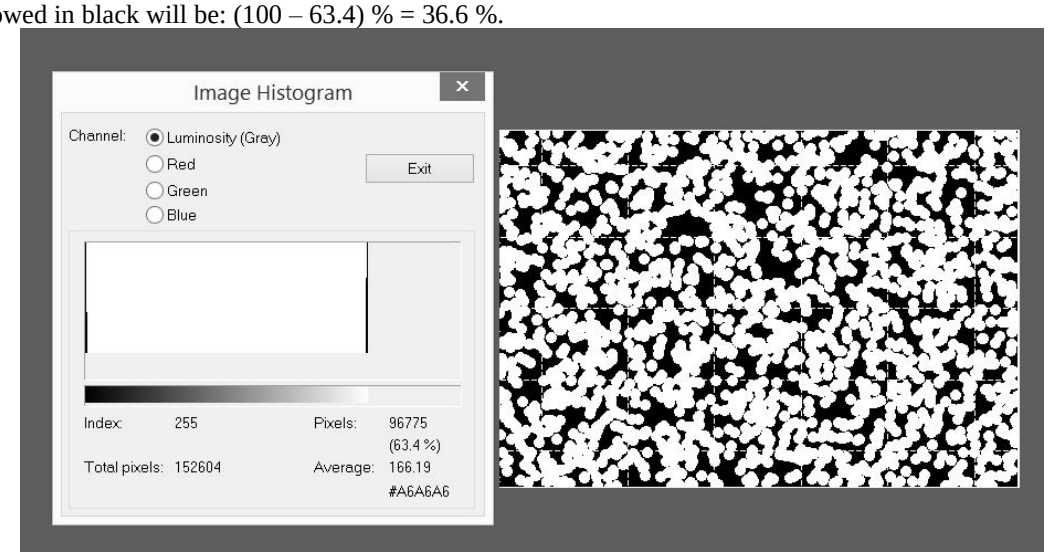

(Source: Authors' elaboration)

The porous body shown in Figure 1 was also simulated by the Monte Carlo method, using stratified random draws (33 random points drawn by grid cell), using the method described by Lopes and Luz (2014) . The relative discrepancy between the two methods was 2.8 %.

Another study with image analysis was conducted by Buckman and collaborators (2017) who also used free software (*ImageJ*) for image processing with subsequent

analysis of the data in *Matlab*. As pointed out by them, this is a low cost alternative with easy operation and quick analysis.

Nabawy (2014), on the other hand, analyzed sandstone images and proposed an equation to predict porosity (expressed in fraction) based on the elongation (***E*** — the length to diameter ratio) of particles:

$$\varepsilon = \frac{0.26188}{E} + 0.21431 \tag{3}$$

Recently, Lopes, Luz and Milhomem have found an equation that describes the surface area of a polydispersed system based on the sharpness parameter of the Rosin–Rammler equation (LOPES; LUZ; MILHOMEM, 2020). On the other hand, Ouchlyama and Tanaka (1986) have estimated the porosity of a bed of particles whose particle size distribution follows the Gaudin-Schumann distribution.

Ideal compaction of a granular medium entails in minimizing the potential energy of the system. That is naturally coming from the principle that a system spontaneously tends to more stable energy states, decreasing its energy. Not taking into account the entropic and steric aspects (cause of granular convection, complex oscillatory phenomena as the so-called Brazilian nut effect and whale effect), the centroid's height evolution as a function of the number of vibration/compaction cycles can be expressed as:

$$z(n) = (z_{\max} - z_{\infty}) \times \exp(-k_{co} \times n) + z_{\infty} \tag{4}$$

Where $\boldsymbol{z_{max}}$ is the initial height (loose height), $\boldsymbol{z_{\infty}}$ is the equilibrium or ultimate height (asymptotic height, after infinite time) and $\boldsymbol{k_{co}}$ is a kinetical parameter (called compacibility) depending on the particles' density, friction coefficient, shape, and surface roughness, besides of the vector acceleration and amplitude of oscillatory movement. Parameter $\boldsymbol{n_c}$ in Equation 4 is the number of vibration cycles (strokes).

Zou *et al.* (2011) performed a similar study, using monodisperse systems, but varying the particle size for each experiment. These authors have showed that the particle size has a strong influence on the porosity value, and the smaller the particle size greater will be its porosity (i.e.: there will be less bed compaction). This behavior has been clearly evidenced for particles smaller than 200 μm, most likely being due to interaction forces,

such as London-van der Waals and Coulomb forces (possibly triboelectric ones, when it comes to dry systems). They also have carried out experiment using mixtures containing two sizes of particles, similar to those by Furnas (1928), with similar results.

Typically, the research about the bulk porosity has been focused primarily on very specific conditions, where there is only one particle size or at most two or three size classes. In real-world conditions what usually happens is a particulate bed that displays a particle size continuous distribution, making the application of these models very complicated and not accurate.

Among the models that have found greater employment in industrial practice in which there is the occurrence of bulk solids, in comparison with the various models, is the Weibull's one (FRERY *et al.*, 2012; KING; SCHNEIDER; KING, 2012; LUZ, 2005).

Chen *et al.* (2018) analyzed the relationship between the Weibull distribution parameters and the compaction of four types of granular material. According to them it was possible to find a good correlation to describe the granular materials.

Burminster (1938 *apud* PERONIUS; SWEETING, 1985) identified the porosity as a function of the size distribution, establishing five types of particulate systems: particles with narrow distribution, particles equally distributed around the mean, particles with bimodal distribution with predominance of coarse fraction or fine, particles showing skewed distribution forward the fine fraction and particles showing skewed distribution forward the coarse fraction. Latham, Munjiza and Lu (2002) reviewed several studies on prediction of porosity in non-spherical particulate systems and they have pointed out is necessary to fit experiments using semi-empirical models (such as the one proposed by Burminster) and numerical models.

Under that same light, in this study we have employed synthetic particulate material, consisting of spheroidal particles, so that the cumulative percent passing (***Y***) versus size (***x***) be reasonably well described by equation Rosin–Rammler–Sperling–Bennett (a special case of Weibull's distribution, and expressed by equation 5) for different sharpness values (***n***) of the equation (2012). The following Equation 5 as a function of the median and sharpness index or modulus (***n***) was gotten by equating 50 % to the cumulative mass fraction through the median opening (x_{50}) followed by a straightforward variable handling.

$$Y = 1 - e^{-\left(\frac{x}{x^*}\right)^n} = 1 - e^{\left[\ln\left(\frac{1}{2}\right) \times \left(\frac{x}{x_{50}}\right)^n\right]} \quad (5)$$

By measuring the porosity in each case mathematical models relating sharpness and porosity can be searched.

Another usual statistical distribution is the Whiten distribution given by Equation 6:

$$Y = \frac{e^{\left[\alpha \times \left(\frac{x}{x_{50}}\right)\right]} - 1}{e^{\left[\alpha \times \left(\frac{x}{x_{50}}\right)\right]} + e^{[\alpha]} - 2} \tag{6}$$

Luz has studied the relationship between the parameter ***n***, sharpness descriptor of the Rosin–Rammler statistical distribution, and the alfa parameter, its counterpart in the Whiten sigmoidal distribution. The results showed that the two parameters are related by the following conversion equation (Equation 7) obtained by non-linear regression analysis, using the computer package *Easyplot* (LUZ, 2005)*:*

$$\alpha = a = 34.555 \times e^{-\left(\frac{3.9}{n^{0.5984}}\right)} \tag{7}$$

According to that author, the previous equation showed excellent precision, for all tested median diameters. Pearson's coefficient of determination (squared regression coefficient) was 99.9 %. With this, it becomes possible to convert, without great loss of information, Whiten's distribution to Rosin–Rammler's distribution, making thereby the eventual equation for predicting the porosity even more general.

2 MATERIALS AND METHODS

Particles used were glass beads (such as those shown in Figure 2) of several sizes. Using spheres (actually spheroids, rather than true geometrical spheres) eliminates the influence of particle shape on the bed porosity. Porosity may also suffer significant influence the container shape due to wall effect. One way to reduce this effect is to use a container with a smaller contact area with bed. It is known that sphere has the least surface area per volume. The container used was a polyethylene terephthalate bottle (vial), spheroidal shape, and with a nominal volume of 0.00025 m^3 (0.25 liter).

Figure 2 — Left: glass beads of class 14 (coarser fraction used in this work); right: sample classified between 74 µm and 150 µm, seen with optical microscopy (scale bar = 100 micrometers).

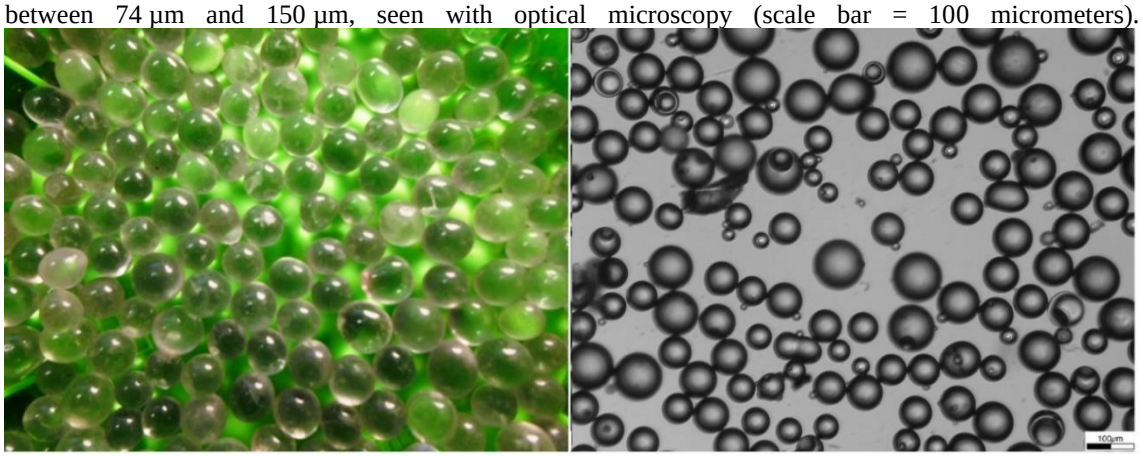

(Source: Authors' personal files)

In order to achieve particle size distribution as close as possible to Weibull–Rosin–Rammler equation, glass beads were sized to obtain beads with narrow size ranges, which were subsequently homogenized in a controlled manner. Screens with different opening sizes are used to perform the separation. At the end 14 size classes were obtained. Table I presents the classes, the upper and lower limiting screens used to get each one, and also the average particle size and the densities of glass beads.

Table I — Particle size and density of glass beads (supplier: Zirtec Company).

Class	Screen range [µm]	Mean size [µm]		Density [kg/m³]	***Class***	Screen range [µm]	Mean size [µm]	Density [kg/m³]
1	53-37	45		2492.2	***8***	590-425	507.5	2509.1
2	75-53	64		2494.4	***9***	840-590	715	2507.4
3	106-75	90.5		2502.3	***10***	1190-840	1015	2502.0
4	150-106	128		2505.1	***11***	1680-1190	1435	2505.0
5	212-150	181		2498.7	***12***	2380-1680	2030	2499.2
6	300-212	256		2513.7	***13***	3350-2380	2865	2495.2
7	425-300	362.5		2511.4	***14***	4760-3350	4055	2500.5

(Source: Authors' elaboration from own experiments and supplier datasheet)

A helium pycnometer from Quantachrome (Ultrapyc model 1200e), based on Boyle–Mariotte law (SHARIF *et al.*, 2015), was used to determine the density of the beads with at least three measures by sample. The solid true density (ρ_s) was determined by using Equation 8.

$$\rho_s = \frac{m_s}{V_s} = \frac{m_s}{V_c - \left(\frac{V_{ex}}{\frac{p_1}{p_2} - 1} \right)} \quad (8)$$

Where: m_s — solid sample mass [kg]; V_s — solid volume [m³]; V_c — volume of the sample chamber [m³]; V_{ex} — volume of the expansion chamber [m³]; p_1 — initial pressure of sample chamber [Pa]; p_2 — equilibrium (final) pressure of sample chamber (and expansion chamber) after valve opening [Pa]. Naturally, an in-built software automatically made the calculations.

In the present work we prefer to quantify the bed mass in analytical balance and then converting its value to volume (by dividing mass by true density), for reproducibility reasons.

The objective of this study was to relate the particle size distribution with porosity. The parameter chosen for the correlation was the sharpness of the Weibull–Rosin–Rammler distribution, n. Using the traditional Weibull–Rosin–Rammler equation (Equation 5) would imply infinity top size. To avoid this algebraic inconsistency, we opted the truncated equation (LUZ, 2017), as shown in Equation 9 below. For convenience a median size (x_{50}) of 362.5 µm and a top size (x_{max}) of 4,055 µm were adopted, according to Equation 9.

$$Y = p(0 \le x \le X < x_{\max}) = 1 - \exp\left[-\left(\frac{\left(\frac{x}{x_{\max} - x} \right)}{x^*} \right)^n \right] = 1 - \exp\left[\ln\left(\frac{1}{2}\right) \times \left(\frac{\left(\frac{x}{x_{\max} - x} \right)}{\left(\frac{x_{50}}{x_{\max} - x_{50}} \right)} \right)^n \right] \quad (9)$$

It was also established that the sharpness values used for the artificial preparation of the required distribution, would be in the range of 0.5 to 3.0, in increments of 0.125. Then, by varying the size (x) and using the average sizes of each class shown in Table I, the cumulative passing fraction of material in this class was calculated. Subtracting this amount from the cumulative passing fraction of the next lower class, the retained fraction of the sample inside that size interval was determined. Of course, this calculation was performed for each value of the sharpness index (n).

It was defined that the quantity of material used for testing was 0.450 kg, after preliminary tests. The mass of each class was determined by multiplying the total mass by the proportion calculated in the previous step. Vibration of the particle bed to obtain greater compaction was not adopted because the system used has revealed size segregation in prospective experiments under vibration. Tests were performed as follows.

First, the required mass of each of the classes was separated. After obtaining the 14 aliquots (corresponding to 14 particle size classes adopted), they were mixed and homogenized.

The homogenized mixture was poured into the measuring container with the aid of a funnel. The container was capped and inverted twenty times. Then, the sample container was placed on the bench, and with tapping and using a glass rod, the top of the bed was smoothed (flattened). Using an overhead transparency pen (fine point) the level of the bed top was marked. The process was repeated three more times, from the container inversion up to the marking of bed level, resulting therefore four density values for each experimental condition.

The spheroidal container (vial) was emptied and cleaned after each set of four measurements. The mass of particulate material used was weighted in balance. From density the actual volume occupied by spheres was obtained. Then the vial was filled with water until one of the marks made with the pen. The mass of water was determined and the process was repeated for each of the remaining marks.

Of course, two volumes are required for determining the porosity: the total volume of particulate bed and volume of voids. The total volume has the same value as the amount of water that filled in the container up to the mark. As the density of water at the test temperature is known water volume was readily calculated, and therefore the total bed volume.

For its part the void volume was determined by the difference between the total bed volume and the actual volume occupied by the particles. Density of the particles was determined with the aid of a gas pycnometer, allowing determination of the particle volume. Having the void volume and total volume of the bed, the porosity was determined, of course, by the division of these two values.

The average volume of particle bed used and their variability are shown in Table II below.

Table II — Statistical parameters of particulate bed volume.

Average volume of particulate bed (V_m):	1.789×10^{-4} m³
Standard deviation (s):	5.001×10^{-7} m³
Coefficient of variation (c.v. = s/V_m):	0.280 %

(Source: Authors' calculation)

By having 84 values of porosity obtained in the experiments, the tool CFTOOL from *Matlab*® was used to approach various regression curves, analyzing, in each case, the overall goodness-of-fit of the model. It was sought thereby to obtain an equation which best foresee the porosity as a function of the sharpness index of the Weibull–Rosin–Rammler distribution.

3 RESULTS

After conducting the test, the following Table (Table III) was prepared from 84 empirical values (four porosity tests for each of the 21 sharpness values). The overall coefficient of variation for the tests was of 3.53 %. In Table III, $\square_m$ is the mean value of porosity, the ratio $s/\square_m$ is its coefficient of variation and z-score is obtained from the division of the deviation of a datum (a raw score) from the population mean by the corresponding standard deviation.

Table III — Summary of results.

n	Porosity (□)				□$_m$	s	s□□$_m$	z-score			
	Test 1	Test 2	Test 3	Test 4	[%]	[%]	[%]	Test 1	Test 2	Test 3	Test 4
0.500	20.76	21.03	20.77	23.77	21.583	1.462	7.01	-0.5618	-0.3808	-0.5522	1.4948
0.625	25.59	23.26	21.89	19.50	22.560	2.551	10.82	1.1881	0.2761	-0.2628	-1.2013
0.750	22.54	22.91	22.10	20.42	21.993	1.098	4.88	0.4975	0.8336	0.0998	-1.4309
0.875	28.36	26.93	26.67	25.81	26.943	1.059	3.88	1.3379	-0.0115	-0.2568	-1.0696
1.000	25.50	26.86	27.60	28.72	27.170	1.353	5.08	-1.2368	-0.2308	0.3213	1.1463
1.125	30.94	27.80	28.23	29.04	29.003	1.394	4.81	1.3932	-0.8662	-0.555	0.0280
1.250	31.65	30.56	30.46	30.36	30.758	0.600	1.94	1.4857	-0.3302	-0.4876	-0.6679
1.375	30.54	31.24	31.72	34.86	32.090	1.908	6.12	-0.8134	-0.4443	-0.1928	1.4505
1.500	29.99	31.84	32.04	32.26	31.533	1.042	3.33	-1.4795	0.2923	0.4911	0.6961
1.625	34.38	34.12	32.22	33.05	33.443	1.001	2.98	0.9402	0.6769	-1.2270	-0.3902
1.750	32.41	32.89	33.11	34.36	33.193	0.834	2.54	-0.9416	-0.3665	-0.0955	1.4036
1.875	36.48	33.04	32.75	32.52	33.698	1.866	5.47	1.4900	-0.3496	-0.5089	-0.6315
2.000	33.97	34.32	34.51	34.67	34.368	0.303	0.88	-1.3213	-0.1598	0.4837	0.9973
2.125	34.42	34.57	34.77	35.75	34.878	0.597	1.73	-0.7686	-0.5112	-0.1752	1.4551
2.250	34.71	35.33	35.53	35.97	35.385	0.521	1.48	-1.2894	-0.1086	0.2816	1.1164
2.375	35.66	35.48	35.19	36.51	35.710	0.569	1.61	-0.0818	-0.4127	-0.9148	1.4093
2.500	37.58	35.35	35.86	36.12	36.228	0.958	2.64	1.4146	-0.9161	-0.3823	-0.1161
2.625	37.41	38.00	35.90	36.21	36.880	0.990	2.67	0.5397	1.1265	-0.994	-0.6721
2.750	34.36	35.12	35.25	35.93	35.165	0.646	1.85	-1.2522	-0.0729	0.1386	1.1864
2.875	37.96	37.30	36.93	36.81	37.250	0.518	1.38	1.3732	0.0958	-0.6200	-0.8490
3.000	37.10	37.58	36.92	37.11	37.178	0.282	0.76	-0.2838	1.4281	-0.9078	-0.2365

(Source: Authors' elaboration from the experiments)

Equation 10 (showed below) was selected after numerous attempts to find an equation with good fit to raw data. This equation results a coefficient of determination $R^2 = 0.9356$.

$$\varepsilon(n) = a \times \left[1 - e^{-\left(\frac{n}{b}\right)^c}\right] + d \tag{10}$$

The values of selected parameters of the equation are shown in Table IV. The second column refers to the regression analysis of cloud 84 Cartesian pairs with the using *Matlab*, whereas third column refers to the analysis of the same 84 points, however using *EasyPlot*. The fourth and last column concerns the regression analysis with *EasyPlot* using the mean porosity values for the 21 experimental conditions (sharpness values).

Table IV — Regression parameters associated with porosity equation.

Parameter		***Matlab*** **(raw data)**	***EasyPlot*** **(raw data)**	***EasyPlot*** **(average)**
a		0.2209	0.2206	0.2204
b		1.1410	1.1417	1.1419
c		1.4370	1.4403	1.4411
d		0.1499	0.1502	0.1503
Coefficient of determination (R^2)		0.9356	0.9356	0.9752
Parameter uncertainty	□(a)	-	0.03849	0.05065
	□(b)	-	0.11511	0.15154
	□(c)	-	0.32173	0.42388
	□(d)	-	0.033426	0.04399
Probability, p-value		1.000000	1.000000	1.000000

(Source: Authors' calculation)

Figure 3 allows the visualization of the results showing the experimental data and the resulting regression curve for porosity of randomly packed of glass beads.

In addition to the high statistical adherence, it is important to consider the porosity when ***n*** tends to infinity. When ***n*** approaches infinity it would be to say the granular medium only contains particles of the same size, so it would be a random packing of spheres of a single diameter. For this case Scott (1960) found porosity value of 0.41 for the system with loose packing and 0.37 for the compacted system. The present model returns the value of 0.3708, indicating goodness-to-fit at that limit.

Figure 3 — Porosity versus sharpness index of Rosin–Rammler equation (circles are raw data, solid triangles are average values).

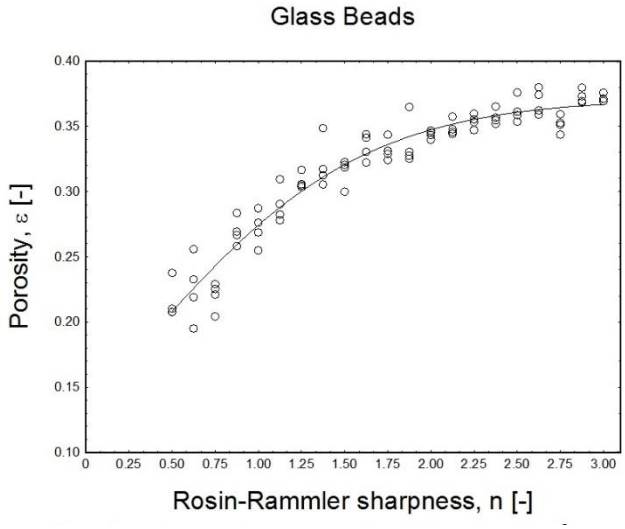

Several other researchers also have carried out experiments of random packing of monosized spheres, obtaining values between 0.37 and 0.40 for the porosity, indicating the model can also predict well those cases where the values of ***n*** are high.

The residual analysis has revealed no structure showing residuals' randomness and therefore the adequacy of the regression equation, albeit with slight tendency to increase dispersion for small values of sharpness, ***n*** (Figure 4). In turn, Figure 5 shows a plot of the predicted values versus the observed values for the dataset.

Figure 4 — Residual analysis for porosity of randomly packed of glass beads.

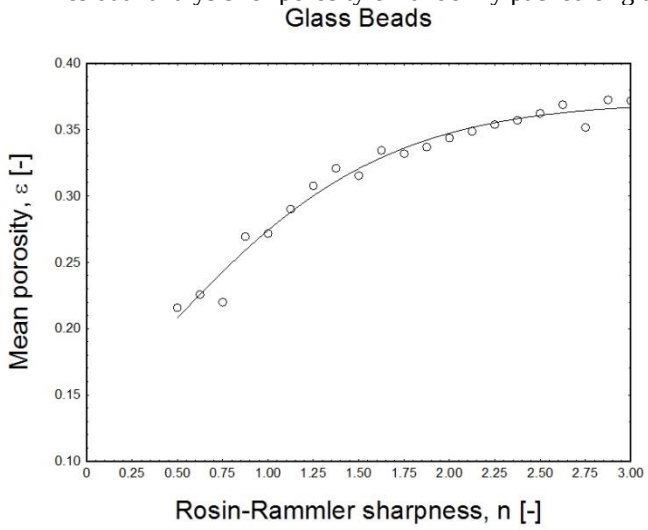

Figure 5 — Predicted porosity versus experimental values.

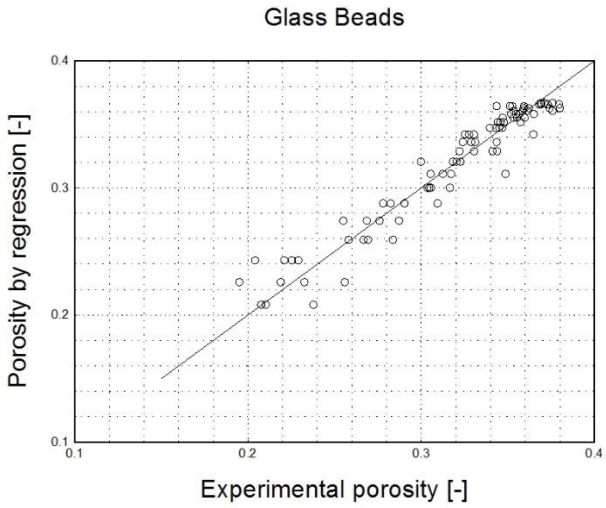

An interesting possibility of applying Equation 10 is in the Ergun equation, which quantifies the head loss due to the percolation of fluid in a particulate bed, widely used in several instances of engineering and given by Equation 11, as a function of particle diameter, ***x***:

$$\frac{\Delta p}{L} = 150\left[\frac{(1-\varepsilon)^2}{\varepsilon^3}\right]\left[\frac{\eta_f}{(\psi x)^2}\right]\left(\frac{Q_{vf}}{A}\right) + 1.75\frac{(1-\varepsilon)}{\varepsilon^3}\frac{\rho_f}{\psi x}\left(\frac{Q_{vf}}{A}\right)^2 \quad (11)$$

Where: Δp is head loss [Pa]; L is the bed thickness [m]; η_f is the fluid dynamic viscosity [Pa.s]; ψ is Wadell sphericity [-]; Q_{vf} is the fluid volumetric flow rate; A is the cross-section area [m^2]; ρ_f is the fluid density [kg/m^3].

Although in principle the equation applies to a monodispersed system, the harmonic mean diameter has been often recommended in the application of the Ergun equation for a polydispersed system. For a particulate system well described by the Rosin–Rammler distribution, Equation 10 can be inserted directly into the Ergun equation, but the problem of calculating the mean harmonic diameter arises.

Thus, working on this line, an empirical relationship was sought between the mean harmonic diameter (x_{har}) and the sharpness index of the distribution (n). For this, using an electronic spreadsheet, the mean harmonic diameters were calculated, varying the abscissa (diameter) between 0.00 and 3.55 (a total of 144 points), for 17 values of sharpness index (with an arbitrary median: x_{50} = 1.000). The non-linear regression of the

Cartesian ordered pairs (n, x_{har}/x_{50}) — illustrated in Figure 6 — allowed the establishment of Equation 12 (with coefficient of determination R^2 = 0.99898) as follows:

$$x_{har} = \left\{1 - e^{-\left(\frac{n}{1.8374}\right)^{1.870}}\right\} x_{50} \tag{12}$$

Figure 6 — Regression of the relative harmonic diameter as a function of n.

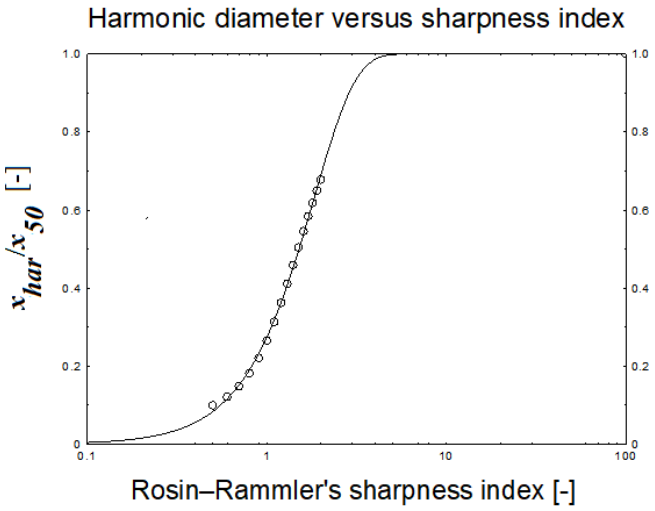

Applying this result in Equation 11 (additionally with the porosity given by Equation 10), a final expression for the specific pressure drop of a granular bed, described by the Rosin–Rammler distribution, results (Equation 13), namely:

$$\frac{\Delta p}{L} = 150\left[\frac{(1-\varepsilon)^2}{\varepsilon^3}\right]\left[\frac{\eta_f}{\left(\psi\left\{1 - e^{-\left(\frac{n}{1.8374}\right)^{1.870}}\right\} x_{50}\right)^2}\right]\left(\frac{Q_{vf}}{A}\right) + 1.75\frac{(1-\varepsilon)}{\varepsilon^3}\frac{\rho_f}{\psi\left\{1 - e^{-\left(\frac{n}{1.8374}\right)^{1.870}}\right\} x_{50}}\left(\frac{Q_{vf}}{A}\right)^2 \tag{13}$$

4 CONCLUSION

Porosity is a fundamental powder and powder mixture property. The non-linear regression equation developed here can be used to predict the value of the porosity of densified spheroidal polydisperse systems ($R^2 \geq 0.97$) if they are reasonably described by Rosin–Rammler distribution. Porosity forecasting of particulate systems described by the

Whiten distribution (a modified logistic one) can also be done, with good accuracy, since Luz equation can be used for converting this kind of distribution to the classical Rosin–Rammler's distribution.

Such statistical predictability of random packing can sometimes eliminate the need for use of complex or expensive methods. Thus, the process control can be improved, as well as its understanding, in numerous applications where this parameter has influence.

A limitation of the presented model is the influence of particle shape, because only spherical glass beads (actually spheroidal particles) have been used in bed formation. But even so, the model can be used as a prediction tool for the minimum porosity value expected in the various processes (as in flotation froths, adsorbent resin packet bed, in situ aquifer evaluation, etc.), in which is extremely difficult or even impossible to obtain an appropriate value for porosity without experimental campaign.

ACKNOWLEDGEMENT

The authors express their gratitude to the Conselho Nacional de Desenvolvimento Científico e Tecnológico (CNPq, the Brazilian council of research and scientific development), Coordenação de Aperfeiçoamento de Pessoal de Nível Superior (CAPES, the Brazilian agency for development of higher education staff), and Fapemig (Research Support Foundation of Minas Gerais). They are also grateful to the and Federal University of Ouro Preto (UFOP) and Vale Institute of Technology (ITV) for their funding of this research.

DECLARATION OF INTEREST

The authors declare no conflict of interest.

REFERENCES

ANDEREGG, F. O. Grading Aggregates II — The application of mathematical formulas to mortars. **Industrial & Engineering Chemistry**, v. 23, n. 9, p. 1058–1064, 1931.

AUGIER, F.; IDOUX, F.; DELENNE, J. Y. Numerical simulations of transfer and transport properties inside packed beds of spherical particles. **Chemical Engineering Science**, v. 65, p. 1055–1064, 2010.

BUCKMAN, J. et al. Quantifying porosity through automated image collection and batch image processing: case study of three carbonates and an aragonite cemented sandstone. **Geosciences**, v. 7, n. 70, 2017.

BURMINSTER, D. M. The grading-density relations of granular materials. **Proc. Am. Soc. Test. Mater.**, v. 38, p. 587– 596, 1938.

BURTSEVA, L. et al. **Multi-sized sphere packings: models and recent approachesFaculty of Mathematics**. Faculty of Mathematics, 21p., 2015.

CAMPELLO, E. M. B.; CASSARES, K. R. Rapid generation of particle packs at high packing rations for DEM simulations of granular compacts. **Latin American Journal of Solids and Structures**, v. 13, p. 23–50, 2016.

CHEN, M.-L. et al. Physical and compaction properties of granular materials with artificial grading behind the particle size distributions. **Advances in Materials Science and Engineering**, 2018.

DAS, S.; DEEN, N. G.; KUIPERS, J. A. M. A DNS study of flow and heat transfer through slender fixed-bed reactors randomly packed with spherical particles. **Chemical Engineering**, v. 160, p. 1–19, 2017.

DAS, S.; RAMARAO, B. V. Inversion of lime mud and papermaking pulp filtration data to determine compressibility and permeability relationships. **Separation and Purification Technology**, v. 28, p. 149–160, 2002.

DIAS, R. et al. Tortuosity variation in a low density binary particulate bed. **Separation and Purification Technology**, v. 51, p. 180–184, 2006.

DORNELAS, V. F. et al. $BaSO_4$ Precipitation impact on the permeability of a pressure porous medium. **Brazilian Journal of Development**, v. 7, n. 5, p. 48877–48893, 2021.

FRERY, A. C. et al. Stochastic particle packing with specified granulometry and porosity. **Granular Matter**, v. 14, n. 1, p. 27–36, 2012.

FURNAS, C. C. **The relations between specific volume, voids, and size composition in systems of broken solids of mixed sizes**. Washington, 1928.

KING, R. P.; SCHNEIDER, C. L.; KING, E. A. **Modeling and Simulation of Mineral Processing Systems, 2nd edition**. SME, 2012.

LANFREY, P.-Y.; KUZELJEVIC, Z. V; DUDUKOVIC, M. P. Tortuosity model for fixed beds randomly packed with identical particles. **Chemical Engineering Science**, v. 65, p. 1891–1896, 2010.

LATHAM, J.-P.; MUNJINZA, A.; LU, Y. On the prediction of void porosity and packing

of rock particulates. **Powder Technology**, v. 125, p. 10–27, 2002.

LOPES, P. F. T.; LUZ, J. A. M. Avaliação estereotômica de teores via método de Monte Carlo. **Holos**, v. 30, n. 3, p. 78–87, 2014.

LOPES, P. F. T.; LUZ, J. A. M.; MILHOMEM, F. O. Specific surface area of polydispersions as a function of size distribution sharpness. **Anais da Academia Brasileira de Ciências**, v. 92, n. 3, 2020.

LUZ, J. A. M. Conversibilidade entre distribuições probabilísticas usadas em modelos de hidrociclones. **Rem: Revista Escola de Minas**, v. 58, n. 1, p. 89–93, 2005.

LUZ, J. A. M. **Fracionamento granulométrico de Sistemas Particulados (notas de aula).** Ouro PretoUFOP, 2017.

MACDONALD, I. F. *et al.* Flow through porous media – the Ergun equation revisited. **Ind. Eng. Chem. Fundam.**, v. 18, p. 199–208, 1979.

MÉDICI, E. F.; ALLEN, J. S. A quantitative technique to compare experimental observations and numerical simulations of percolation in thin porous materials. **Transp. Porous Med.**, v. 115, p. 435–447, 2016.

MONTENEGRO-BALAREZO, F. J.; LUZ, J. A. M.; PEREIRA, C. A. Emprego de argamassa expansiva e termoconsolidação de peças em cantaria. **REM: R. Esc. Minas**, v. 56, n. 3, p. 161–167, 2003.

MOTA, M.; TEIXEIRA, J. A.; YELSHIN, A. Image analysis of packed beds of spherical particles of different sizes. **Separation and Purification Technology**, v. 15, p. 59–68, 1999.

MUELLER, G. E. A simple method for determining sphere packed bed radial porosity. **Powder Technology**, v. 229, p. 90–96, 2012.

NABAWY, B. S. Estimating porosity and permeability using digital image analysis (DIA) technique for highly porous sandstones. **Arabian Journal of Geosciences**, v. 7, p. 889–898, 2014.

OUCHLYAMA, N.; TANAKA, T. Porosity estimation from particle size distribution. **Industrial and Engineering Chemistry Fundamentals**, v. 25, n. 1, p. 125–129, 1986.

PERONIUS, N.; SWEETING, T. J. On the correlation of minimum porosity with particle size distribution. **Powder Technology1**, v. 42, p. 113–121, 1985.

PÖTTKER, W. E.; APPOLONI, C. R. **Medida da porosidade de materiais amorfos por transmissão de raios gama**. INAC 2000 — V ENAN. **Anais**.

POZZOBON, V.; COLIN, J.; PERRÉ, P. Hydrodynamics of a packed bed of non-spherical polydisperse particles: A fully virtual approach validated by experiments. **Chemical Engineering Journal**, v. 354, p. 126–136, 2018.

PRIOR, J. M. V; ALMEIDA, I.; LOUREIRO, J. M. Prediction of the packing porosity of mixtures of spherical and non-spherical particles with a geometric model. **Powder Technology2**, v. 249, p. 482–496, 2013.

RODRÍGUEZ, J.; ALLIBERT, C. H.; CHAIX, J. M. A computer method for random

packing of spheres of unequal size. **Powder Technology**, v. 47, p. 25–83, 1986.

SCHMIDT, E.; LÖFFLER, F. Preparation of dust cakes for microscopic examination. **Powder Technology**, v. 60, n. 2, p. 173–177, 1990.

SCOTT, G. D. Packing of spheres: packing of equal spheres. **Nature**, v. 188, n. 4754, p. 908–909, 1960.

SHARIF, S. et al. A simplified approach to determine effective surface area and porosity of low bulk density active pharmaceutical ingredients in early development. **Advanced Powder Technology**, v. 26, p. 337–348, 2015.

SILVA, D. A. E; GEYER, A. B.; PANTOJA, J. C. Porosidade do concreto versus forma do agregado graúdo. **Brazilian Journal of Development**, v. 6, n. 8, p. 60359–60376, 2020.

TRASK, P. D.; HAMMAR, H. E.; WU, C. C. **Origin and Environment of source sediments of petroleum**. Houston: Gulf Publishing Co., 1932.

WANG, Y.; HERDEGEN, V.; REPKE, J.-U. Numerical study of different particle size distribution for modelling of solid-liquid extraction in randomly packed beds. **Separation and Purification Technology**, v. 171, p. 131–143, 2016.

ZOU, R. P.; GAN, M. L.; YU, A. B. Prediction of the porosity of multi-component mixtures of cohesive and non-cohesive particles. **Chemical Engineering Science**, v. 66, n. 20, p. 4711–4721, 2011.